



This is a self-archived version of an original article. This version may differ from the original in pagination and typographic details.

Author(s): Ge, Z.; Eronen, T.; Ramalho, M.; de Roubin, A.; Nesterenko D., A.; Kankainen, A.; Beliuskina, O.; de Groote, R.; Geldhof, S.; Gins, W.; Hukkanen, M.; Jokinen, A.; Koszorús, Á.; Kotila, J.; Kostensalo, J.; Moore I., D.; Pirinen, P.; Raggio, A.; Rinta-Antila, S.; Sevestrean V., A.; Suhonen, J.; Virtanen, V.; Zadvornaya, A.

Title: Direct high-precision measurement of the mass difference of ^{77}As – ^{77}Se related to neutrino mass determination

Year: 2024

Version: Published version

Copyright: © The Author(s) 2024

Rights: CC BY 4.0

Rights url: <https://creativecommons.org/licenses/by/4.0/>

Please cite the original version:

Ge, Z., Eronen, T., Ramalho, M., de Roubin, A., Nesterenko D., A., Kankainen, A., Beliuskina, O., de Groote, R., Geldhof, S., Gins, W., Hukkanen, M., Jokinen, A., Koszorús, Á., Kotila, J., Kostensalo, J., Moore I., D., Pirinen, P., Raggio, A., Rinta-Antila, S., . . . Zadvornaya, A. (2024). Direct high-precision measurement of the mass difference of ^{77}As – ^{77}Se related to neutrino mass determination. *European Physical Journal A*, 60(5), Article 104.
<https://doi.org/10.1140/epja/s10050-024-01317-3>



Direct high-precision measurement of the mass difference of ^{77}As – ^{77}Se related to neutrino mass determination

Z. Ge^{1,a}, T. Eronen^{1,b}, M. Ramalho^{1,c}, A. de Roubin^{2,3}, D. A. Nesterenko¹, A. Kankainen¹, O. Beliuskina¹, R. de Groot^{1,3}, S. Geldhof^{1,11}, W. Gins¹, M. Hukkanen^{1,2}, A. Jokinen¹, Á. Koszorús^{4,3}, J. Kotila^{5,6,7}, J. Kostensalo⁸, I. D. Moore¹, P. Pirinen¹, A. Raggio¹, S. Rinta-Antila¹, V. A. Sevestrean^{7,9,10}, J. Suhonen^{1,7,d}, V. Virtanen¹, A. Zadvornaya^{1,12}

¹ Department of Physics, University of Jyväskylä, P.O. Box 35, 40014 Jyväskylä, Finland

² Centre d'Etudes Nucléaires de Bordeaux Gradignan, UMR 5797 CNRS/IN2P3, Université de Bordeaux, 19 Chemin du Solarium, CS 10120, 33175 Gradignan Cedex, France

³ Present address: KU Leuven, Instituut voor Kern-en Stralingsfysica, 3001 Leuven, Belgium

⁴ Department of Physics, University of Liverpool, Liverpool L69 7ZE, UK

⁵ Finnish Institute for Educational Research, University of Jyväskylä, P.O. Box 35, 40014 Jyväskylä, Finland

⁶ Center for Theoretical Physics, Sloane Physics Laboratory Yale University, New Haven, CT 06520-8120, USA

⁷ International Centre for Advanced Training and Research in Physics, P.O. Box MG12, 077125 Bucharest-Măgurele, Romania

⁸ Natural Resources, Natural Resources Institute Finland, Yliopistonkatu 6B, 80100 Joensuu, Finland

⁹ Faculty of Physics, University of Bucharest, 405 Atomiștilor, P.O. Box MG11, 077125 Bucharest-Măgurele, Romania

¹⁰ "Horia Hulubei" National Institute of Physics and Nuclear Engineering, 30 Reactorului, POB MG-6, 077125 Bucharest-Măgurele, Romania

¹¹ Present address: GANIL, CEA/DSM-CNRS/IN2P3, Bd Henri Becquerel, 14000 Caen, France

¹² Present address: University of Edinburgh, Edinburgh EH9 3FD, UK

Received: 5 February 2024 / Accepted: 12 April 2024

© The Author(s) 2024

Communicated by Klaus Blaum

Abstract The first direct determination of the ground-state-to-ground-state β^- -decay Q -value of ^{77}As to ^{77}Se was performed by measuring their atomic mass difference utilizing the double Penning trap mass spectrometer, JYFLTRAP. The resulting Q -value is 684.463(70) keV, representing a remarkable 24-fold improvement in precision compared to the value reported in the most recent Atomic Mass Evaluation (AME2020). With the significant reduction of the uncertainty of the ground-state-to-ground-state Q -value and knowledge of the excitation energies in ^{77}Se from γ -ray spectroscopy, the ground-state-to-excited-state Q -value of the transition $^{77}\text{As} (3/2^-, \text{ground state}) \rightarrow {}^{77}\text{Se}^* (5/2^+, 680.1035(17) \text{ keV})$ was refined to be 4.360(70) keV. We confirm that this potential low Q -value β^- -decay transition for neutrino mass determination is energetically allowed at a confidence level of about 60σ . Nuclear shell-model calculations with two well-established effective Hamiltonians were used to estimate the partial half-life for the low Q -value transition. The half-life was found to be of the order of 10^9 years for this first-

forbidden non-unique transition. Since the half-life of ^{77}As is only ≈ 2 days, usage of it as source for rare-event experiments searching for the electron antineutrino mass would be challenging.

1 Introduction

The discovery of neutrino oscillations has challenged the idea of massless neutrinos, thus requiring extension of the Standard Model to account for neutrino mass [1–3]. Neutrino oscillations provide the possibility to infer the neutrino-mass splittings to a high precision. However, they are not sensitive to the absolute neutrino-mass scale, e.g., the mass of the lightest mass eigenstate. To access the absolute mass scale, three complementary approaches are currently being explored: neutrinoless double- β decay, cosmological observations, and kinematic studies of weak-interaction processes such as single β^\pm decays and electron capture (EC) [4–8]. Among them, high-precision measurements of single β^\pm decays or EC are considered to be the most model-independent methods to determine the absolute scale of the (anti)neutrino mass, as they require no prior assumption on the basic nature (Dirac vs. Majorana) of the neutrino.

^a e-mail: zhuang.z.ge@jyu.fi (corresponding author)

^b e-mail: tommi.eronen@jyu.fi (corresponding author)

^c e-mail: madeoliv@jyu.fi (corresponding author)

^d e-mail: jouni.t.suhonen@jyu.fi (corresponding author)

The neutrino mass can be determined by comparing the measured and the expected endpoint energy (Q_β). The presence of a finite neutrino mass causes a shift in the decay endpoint and alters the shape of the decay spectrum, particularly in the proximity of the endpoint. For β decays, the fraction of decay events that fall into an energy interval just below the endpoint energy is proportional to Q_β^{-3} [9], while for EC the proportionality of the event fraction to Q_β can be even steeper. This implies that nuclear transitions with the lowest possible Q -value are desirable [9]. Currently, two nuclei ${}^3\text{H}$ (β^- decay) and ${}^{163}\text{Ho}$ [10,11] (EC), with low ground-state-to-ground-state (gs-to-gs) decay Q values of 18.59201(7) keV [12], and 2.8632(6) keV [10,11,13], are employed for long-term direct neutrino-mass measurements [8] in experiments such as KATRIN (KArlsruhe TRitium Neutrino) [14,15], ECHo (Electron Capture in ${}^{163}\text{Ho}$) [7,16–18], Project 8 [19] and HOLMES [20,21].

Further explorations for nuclear β -decay or EC transitions with low Q values are desirable for prospective (anti)neutrino mass determination experiments [22–25]. One transition of interest is the β^- transition ${}^{77}\text{As}$ ($3/2^+$, 38.790(50) h) \rightarrow ${}^{77}\text{Se}^*$ ($5/2^-$, $E^* = 680.1035(17)$ keV) due to its small gs-to-es state Q^* ($Q - E^*$) value of 3.1(17) keV. The Q^* value can be deduced from the high-precision excitation-energy E^* evaluation [26], with sub-keV precision, and the gs-to-gs Q value of 683.2(17) keV from AME2020 [27,28], which provides the main uncertainty of Q^* . The gs-to-gs Q value of ${}^{77}\text{As}$ in AME2020 is evaluated from reaction and β^- -decay data of ${}^{80}\text{Se}(\text{p},\alpha){}^{77}\text{As}$, ${}^{76}\text{Ge}({}^3\text{He},\text{d}){}^{77}\text{As}$, and ${}^{77}\text{As}(\beta^-){}^{77}\text{Se}$, with influence of 32%, 31.8%, and 17.9%, respectively.

Recent and thorough investigations into possible low Q -value β^- -decay and EC candidate transitions have employed the Penning-trap mass spectrometry (PTMS) technique [29–41], highlighting the importance of high-precision direct Q -value measurements prior to utilisation of these nuclei in long-term (anti)neutrino-mass measurements. These earlier investigations have revealed significant discrepancies (exceeding 10 keV) between Q values obtained through indirect methods, such as reaction and decay spectroscopy, compared to those derived from direct mass measurements. This inconsistency spans a wide range of mass numbers, see e.g. Refs. [32,41,42].

In this work, we report on the first direct gs-to-gs β^- -decay Q -value measurements of ${}^{77}\text{As}$ with the JYFLTRAP double PTMS at the University of Jyväskylä [43–45]. The Q -value of the transition to the excited state of interest is evaluated and determined with a high precision. Moreover, the half-life of the candidate transition is assessed based on nuclear shell-model calculations in order to validate the possibility of using ${}^{77}\text{As}$ for future long-term antineutrino-mass determination experiments.

2 Experimental description

The direct measurement of the Q value, based on mass difference measurements of the decay pair ions of ${}^{77}\text{As}^+$ and ${}^{77}\text{Se}^+$, was carried out at the Ion Guide Isotope Separator On-Line facility (IGISOL) using the JYFLTRAP double Penning trap mass spectrometer [43], situated at the University of Jyväskylä [44,45]. To produce the ions of interest at IGISOL, a 9-MeV deuteron beam from the K-130 cyclotron was directed onto a thin germanium target with a thickness of approximately 2 mg/cm². Ions of ${}^{77}\text{As}^+$ and ${}^{77}\text{Se}^+$ were simultaneously produced through fusion-evaporation reaction. These produced ions were stopped in the gas cell of the IGISOL light-ion ion guide [46] by colliding with high-purity helium gas at a pressure of about 100 mbar. During this process, the highly charged ions undergo recombination, predominantly adopting a singly charged state. The resulting recoils exited the gas cell through a small nozzle into a sextupole ion guide (SPIG) [47], which transports the ions into high vacuum and a subsequent electrode system accelerates them to an energy of 30 keV. A dipole magnet with a mass resolving power of approximately 500 adequately isolates only the isobaric ions with $A = 77$, where A represents the mass number. Following the separation, the mass-number-selected ions were transported through an electrostatic switchyard housing a fast kicker electrode used to chop the beam for an optimum number of ions. The ions were then injected into a radiofrequency quadrupole (RFQ) cooler-buncher [48], which cooled and bunched the beam. Finally, the resulting bunches were transported to the JYFLTRAP double Penning trap for the actual frequency ratio measurement.

The JYFLTRAP double Penning trap comprises two cylindrical traps located in a 7-T superconducting magnet, as illustrated schematically in Fig. 1a. The cooled and bunched ions are confined using the combination of a homogeneous magnetic field and a quadrupolar electrostatic potential inside the traps, where they undergo the superposition of three simple harmonic modes, one axial and two radial. The first trap, designated as the preparation trap, serves as a high-resolution mass separator. In contrast, the second trap, referred to as the measurement trap, is utilized for finely detailed mass determination using ion-cyclotron-resonance techniques.

The ion beam contained ${}^{77}\text{Ge}^+$ as a co-produced impurity. In the first trap, an isobarically purified sample of ions was prepared using the mass-selective buffer gas cooling method [49], providing a typical resolving power $M/\Delta M \approx 10^5$. This method was sufficient to provide a clean sample of ${}^{77}\text{Se}^+$ or ${}^{77}\text{As}^+$ ions.

The determination of the gs-to-gs Q ($Q_{\beta^-}^0$) value is based on the measurement of the cyclotron frequency, $v_c = \frac{1}{2\pi} \frac{q}{m} B$, where q/m is the charge-to-mass ratio of the stored ion and

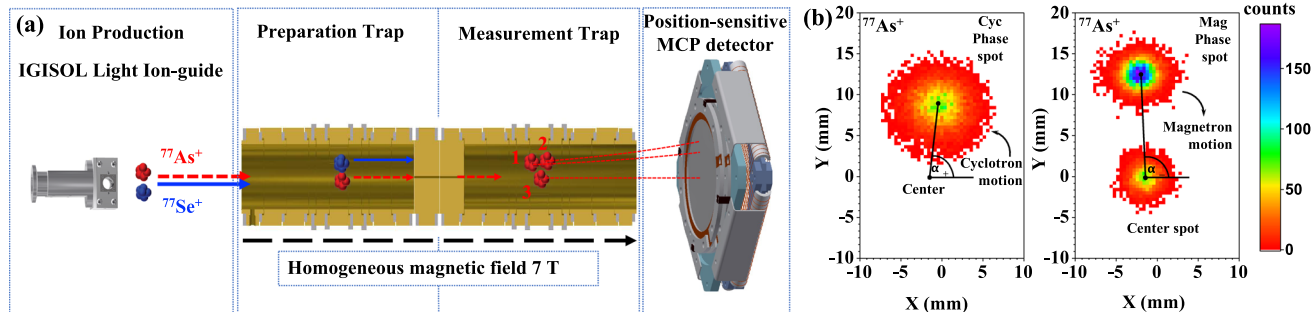


Fig. 1 **a** Schematic view of ion production and mass measurements using the PI-ICR technique at IGISOL. The $^{77}\text{As}^+$ and $^{77}\text{Se}^+$ ions were produced from the fusion reaction with a 9-MeV deuteron beam from K130 cyclotron, bombarding a germanium target of approximately 2 mg/cm^2 in thickness. Ions having mass number of 77 were selected with a dipole magnet and transported to the JYFLTRAP PTMS for final ion species selection in the preparation trap by means of a buffer-gas cooling technique and cyclotron frequency determination using the phase-imaging technique in the measurement trap. A position-sensitive

MCP detector was used to register the images of the motion phases. **b** An illustration of the radial-motion ("magnetron", "cyclotron", and "center") projection of the $^{77}\text{As}^+$ ions onto the position-sensitive MCP detector. The cyclotron phase spot is displayed on the left side and the magnetron phase spot on the right. The angle difference between the two spots relative to the center spot is utilized to deduce the cyclotron frequency of the measured ion. The color bar indicates the number of ions in each pixel

B is the magnetic field strength, for both the decay parent and decay daughter ions. In this work, the phase-imaging ion-cyclotron-resonance (PI-ICR) technique [50,51] was employed for measuring the cyclotron frequencies. Specifically, measurement scheme number 2 described in [52] was utilized for directly measuring the cyclotron frequency.

Two timing patterns, denoted as "magnetron" and "cyclotron", were employed (see Refs. [50,51] for detailed information). These patterns were nearly identical, differing only in the initiation moment of the π -pulse that converts the ions' cyclotron motion to magnetron. In the "magnetron" pattern, ions primarily circulated in the trap with magnetron motion for a duration t_{acc} (accumulation time), while in the "cyclotron" pattern, ions revolved with cyclotron motion. These patterns produced magnetron and cyclotron spots or phases on the position-sensitive micro-channel plate (MCP) detector located after the trap, as illustrated in Fig. 1a. The patterns enable the calculation of the angle between the phases of cyclotron and magnetron motion with respect to the center spot, $\alpha_c = \alpha_+ - \alpha_-$, where α_+ and α_- are the polar angles of cyclotron and magnetron phases, respectively. The acquired "magnetron" and "cyclotron" phase positions of $^{77}\text{As}^+$ ions are depicted in the left and right panels of Fig. 1b. It is essential to determine the position of the motional center spot, also shown in Fig. 1b.

Finally, the cyclotron frequency ν_c is deduced from:

$$\nu_c = \frac{\alpha_c + 2\pi n_c}{2\pi t}, \quad (1)$$

where n_c is the number of complete revolutions of the ions during the phase accumulation time t_{acc} . The measurement procedure ensured that α_c remained small to reduce system-

atic shifts caused by image distortion. To achieve this, the duration t_{acc} was selected to closely align with integer multiples of the ν_c period. This minimized the angle α_c , ensuring minimal impact from the interconversion of magnetron and cyclotron motions [52,53]. During the measurements, α_c did not exceed a few degrees.

Two different accumulation times (330 and 321 ms) for both $^{77}\text{Se}^+$ and $^{77}\text{As}^+$ ions during the measurement were used. The chosen duration t_{acc} ensured the separation of the cyclotron spot of the target ion from any potential isobaric, isomeric, or molecular contaminants. The delay of the initiation of the π pulse was repeatedly scanned over one magnetron period and the final extraction delay was varied over one cyclotron period to account for any residual magnetron and cyclotron motion that could shift the different spots. This constituted in a total of $5 \times 5 = 25$ scan points for both magnetron and cyclotron phase spots.

The $Q_{\beta^-}^0$ value is directly obtained through the cyclotron frequency ratio, $R = \nu_{c,\text{Se}}/\nu_{c,\text{As}}$, where $\nu_{c,\text{As}}$ is the cyclotron frequency for $^{77}\text{As}^+$ and $\nu_{c,\text{Se}}$ for $^{77}\text{Se}^+$. During this experiment, alternating measurements of the $^{77}\text{As}^+$ and $^{77}\text{Se}^+$ cyclotron frequency measurements were conducted every few minutes to minimize the contribution of magnetic field fluctuations in the measured cyclotron frequency ratio. Still, linear interpolation was employed to determine the magnetic field at the moment of the parent cyclotron frequency measurement. The $Q_{\beta^-}^0$ value, mass difference of ^{77}As and ^{77}Se , can be given as:

$$Q_{\beta^-} = (M_p - M_d)c^2 = (R - 1)(M_d - qm_e)c^2 + (R \cdot B_d - B_p), \quad (2)$$

where M_p and M_d are the atomic masses of the parent (^{77}As) and daughter (^{77}Se), respectively. m_e denotes the mass of an electron, and R represents the cyclotron frequency ratio ($\frac{\nu_{c,d}}{\nu_{c,p}}$) for singly charged ions ($q = 1$). The electron binding energies of the parent and daughter atoms are denoted as B_p (9.78855(25) eV) and B_d (9.752390(15) eV) [54]. Since both the parent and daughter, as mass doublets, have the same A/q , the mass-dependent error becomes effectively negligible compared to the statistical uncertainty achieved in the measurement [55]. Moreover, due to the fact that the mass difference of the parent and daughter is very small ($\Delta M/M < 10^{-4}$), the contribution from the reference (daughter) mass uncertainty of 0.06 keV/c² is suppressed by that factor and thus can be disregarded.

3 Results and discussion

The data collection involved initiating a ν_c measurement of $^{77}\text{Se}^+$ for four full scan rounds (one round consisting of 5×5 points for both magnetron and cyclotron phases), followed by the measurement of $^{77}\text{As}^+$ for four full scan rounds. Subsequently, a center spot was recorded with $^{77}\text{Se}^+$ ions. In total, these steps lasted about 7 min and were repeated. For each repetition, the positions of each spot were determined using the maximum likelihood method and the phase angles were calculated to deduce the cyclotron frequencies [32, 50, 51]. The consecutive fitted cyclotron frequencies of $^{77}\text{Se}^+$ were linearly interpolated to the time of the measurement of $^{77}\text{As}^+$. This interpolated frequency was used to deduce the cyclotron resonance frequency ratio R . The contribution of temporal fluctuations of the magnetic field to the final frequency ratio uncertainty was less than 10^{-10} since the frequency measurements of the ion pair were tightly interleaved. The incident ion rate was limited to a maximum of 5 detected ions/bunch with the median value being around 2 ions/bunch. Bunches containing more than 5 ions were excluded from the analysis to mitigate a potential cyclotron frequency shift due to ion-ion interactions [55, 56]. Count-rate class analysis [56] was employed to verify that the frequency indeed did not shift. By maintaining a small angle $\alpha_c < 10$ degrees during the measurements, the frequency shifts due to ion image distortions remained well below the statistical uncertainty. The total measurement period spanned 13.1 h, which we divided into four time slots: 7.2, 3.7, 0.6, and 1.6 h as shown in Fig. 2. This division allowed us to maintain the desired small angle of α_c . The weighted mean ratio \bar{R} of the single ratios was computed alongside the inner and outer errors. The maximum of the inner and outer errors of the Birge ratios [57], was adopted as the weights to calculate the final weighted mean cyclotron frequency ratio \bar{R} . The final frequency ratio \bar{R} and the resultant $Q_{\beta^-}^0$ -values are 1.000

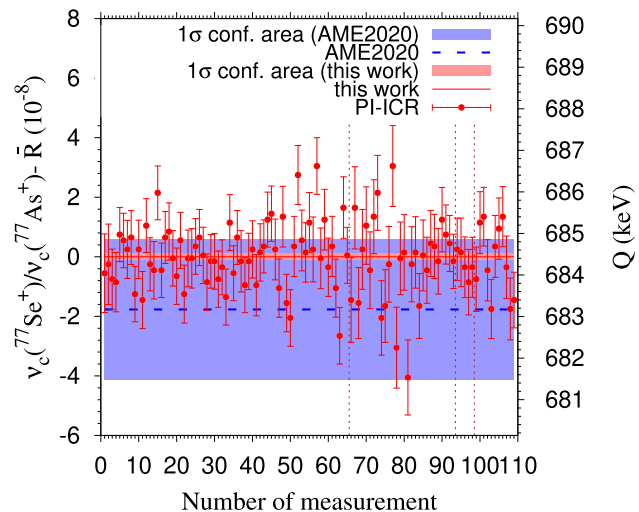


Fig. 2 The measured cyclotron frequency ratios R ($\nu_c(^{77}\text{Se}^+)/\nu_c(^{77}\text{As}^+)$) (left axis) and Q value (right axis) in this work compared to evaluated values from AME2020. The red dots with uncertainties are the measured PI-ICR single ratios in four time slots, which are separated with vertical brown dashed lines. The weighted average value in this work $\bar{R} = 1.000\,009\,552\,87(98)$ is represented by the solid red line and its 1σ uncertainty band is shaded in red. The dashed blue line indicates the value adopted from AME2020 with its 1σ uncertainty area shaded in blue. The first subset of data was acquired with an accumulation time of 330 ms, while the other subsets were obtained using an accumulation time of 321 ms. The Birge ratios for these subsets are 1.07, 1.20, 0.46, and 1.14

009 552 87(98) and 684.463(70) keV, respectively. In Fig. 2, the results of the analysis are contrasted with the literature values.

The $Q_{\beta^-}^0$ value of ^{77}As from this work is a factor of 24 more precise and 1.3(17) keV larger than the value in AME2020 [28]. The mass-excess value of ^{77}As was deduced to be $-73915.026(94)$ keV/c² and the precision was improved by a factor of 18. The uncertainty of the mass excess for ^{77}As has an additional 0.06 keV/c² uncertainty in the mass of the daughter ^{77}Se as reference, which was evaluated based on (n,γ) reaction experiments [58–60] in AME2020 [27, 28]. Combining the new $Q_{\beta^-}^0$ value together with the nuclear energy level data gives the final Q -values for decays to the potential low Q -value states, as tabulated in Table 1 and illustrated in Fig. 3. The gs-to-es $Q_{\beta^-}^*$ value of 4.360(70) keV for the decay channel $^{77}\text{As} (3/2^-) \rightarrow ^{77}\text{Se} (5/2^+, 680.1035(17) \text{ keV})$, is comparable to the presently running direct neutrino mass experiments using electron-capture decaying ^{163}Ho with a Q value of 2.8632(6) keV [13].

The transition of interest is first-forbidden non-unique (1st FNU) and thus depends on nuclear structure through nuclear matrix elements (NME). To compute these NME and to estimate the half-life of this transition, nuclear shell-model (NSM) calculations utilizing the software *KSHELL* [61], with the well established effective interactions *jj44bpn* [62] and

Table 1 Transition from the ground state of the parent nucleus ^{77}As to the excited state of the daughter ^{77}Se . The first and second columns illustrate the experimental spin-parity of the initial ground state and its half-life. The third column gives the measured spin-parity of the excited final state. The fourth column gives the decay type, which in this case is first-forbidden non-unique (first FNU). The fifth column gives the gs-to-

gs decay Q -value ($Q_{\beta^-}^0$) from AME2020 [27,28] and the sixth column from this work. The seventh and eighth columns give the gs-to-es decay Q value ($Q_{\beta^-}^*$) from the literature [27] and this work, respectively. The ninth column lists the level of being positive/negative (in σ). The last column gives the excitation energy E^* from [26]. All the energy values are in units of keV

Initial state	Half-life	Final state	Decay type	$Q_{\beta^-}^0$ (AME2020)	$Q_{\beta^-}^0$ (this work)	$Q_{\beta^-}^*$ (AME2020)	$Q_{\beta^-}^*$ (this work)	$Q/\delta Q$ (this work)	E^*
^{77}As ($3/2^-$)	38.790(50) h	^{77}Se ($5/2^+$)	First FNU	683.2(17)	684.463(70)	3.1(17)	4.360(70)	62	680.1035(17)

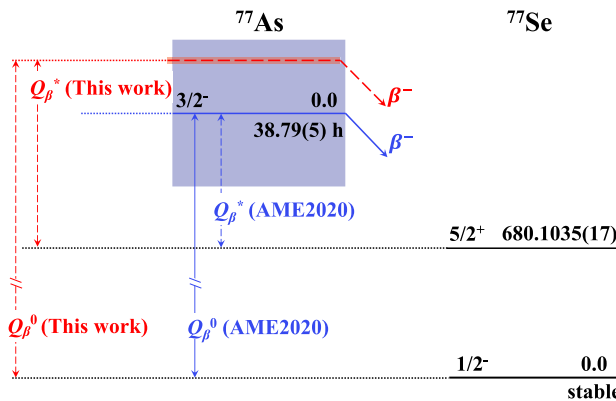


Fig. 3 The transition of ^{77}As ground-state β^- decay to the 680.1035(17) keV $5/2^+$ state in ^{77}Se . The horizontal blue line depicts the level with the $Q_{\beta^-}^0$ taken from AME2020 [27,28] (shaded area shows the 1σ uncertainty) and the red dashed line the $Q_{\beta^-}^0$ from this work. The data for the level scheme are adopted from [26]

excitation energies are generally in fair agreement with the evaluation data.

The dependence of the partial half-life of the $3/2^- \rightarrow 5/2^+$ transition on the Q value is shown in Fig. 4. The computations of the β^- transition rate account for screening, radiative, and atomic exchange corrections. The atomic exchange correction was originally derived for allowed β decays by Nitescu et al. [64] and is the most important contribution due to the low Q value of the discussed transition, as can be seen in Fig. 4. The computed half-life is of the order of 10^9 years for this first FNU transition, which rules out this candidate to be a potential source for rare-event experiments searching for the electron antineutrino mass. Due to the short half-life (less than 2 days) of the isotope ^{77}As , it poses additional challenges for inclusion in a long-term neutrino mass determination experiment.

jun45pn [63], were performed. Their model spaces consist of adopting ^{56}Ni as a closed core with the orbitals $0f_{5/2}$, $1p_{3/2}$, $1p_{1/2}$, and $0g_{9/2}$ for both protons and neutrons. We assess the reliability of the nuclear Hamiltonians employed by analyzing the magnetic dipole and electric quadrupole moments, alongside the excitation energies, predicted by the models in Table 2. The computed electromagnetic properties and the

Table 2 Comparison of the experimental and *jj44bpn* and *jun45pn*-computed state energies E_{exc} (in units of MeV), electric quadrupole moments Q_e (in units of barn), and magnetic dipole moments μ (in units of nuclear magneton μ_N). The experimental evaluation data are

Experimental evaluation				<i>jj44bpn</i>			<i>jun45pn</i>		
Isotope (J^π)	E_{exc} (MeV)	Q_e (barn)	μ (μ_N)	E_{exc} (MeV)	Q_e (barn)	μ (μ_N)	E_{exc} (MeV)	Q_e (barn)	μ (μ_N)
^{77}As ($3/2^-$)	0.000	–	+ 1.2940(13)	0.000	+0.2626	+ 1.4775	0.000	+ 0.2447	+ 1.9403
^{77}As ($5/2^-$)	0.264	–	+ 0.74(2)	0.265	-0.0899	+ 0.9456	0.212	-0.0488	+ 0.4737
^{77}Se ($1/2^-$)	0.000	–	+ 0.53356(5)	0.000	–	+ 0.5667	0.168	–	+ 0.5959
^{77}Se ($5/2^-$)	0.250	+ 0.76(5)	+1.12(3)	0.486	-0.1378	+ 0.4319	0.337	+ 0.376	+1.3252
^{77}Se ($5/2^-$)	0.439	–	+ 1.0(3)	0.665	+ 0.2128	+ 1.2053	0.677	-0.1671	+ 0.7419
^{77}Se ($5/2^+$)	0.680	–	–	0.561	-0.3902	-0.9399	0.635	-0.4334	-1.0071

from [26]. Effective charges adopted are $e_{\text{eff}}^p = 1.5e$ and $e_{\text{eff}}^n = 0.5e$ and the bare g-factors are $g_I(p) = 1$, $g_I(n) = 0$, $g_S(p) = 5.585$, and $g_S(n) = -3.826$

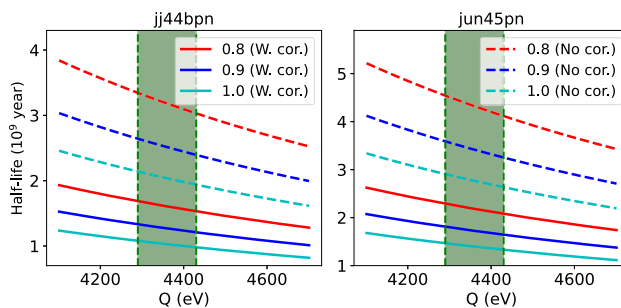


Fig. 4 Computed partial half-lives as a function of available energy (Q value) for the transition ^{77}As ($3/2^-$) \rightarrow ^{77}Se ($5/2^+$) for different choices of the axial-vector coupling g_A (0.8, 0.9 and 1.0) using the effective Hamiltonians $\text{jun}45\text{pn}$ (left panel) and $\text{jun}45\text{pn}$ (right panel). The legend includes half-life values with (W.) and without (No) the atomic exchange correction (cor.). Additionally, green vertical dashed lines shaded in between with green color denote the highest and lowest available energies derived in this work for the transition, which are 4.430 and 4.290 keV, respectively

Q -value is in good agreement with the evaluated value in AME2020 but its uncertainty was improved by a factor of 24. The candidate FNU transition ^{77}As ($3/2^-$) \rightarrow ^{77}Se ($5/2^+$, 680.1035(17) keV) is confirmed to be energetically allowed at a level of more than 60σ . Furthermore, the newly derived gs-to-es Q value allowed us to quantify the order of magnitude of the partial half-life of this transition by using nuclear wave functions obtained with the use of two different established Hamiltonians in nuclear shell-model calculations. The obtained half-life of approximately 10^9 years for this first FNU transition, excludes ^{77}As as a viable candidate for future long-term neutrino mass determination experiments.

Acknowledgements We acknowledge the staff of the Accelerator Laboratory of University of Jyväskylä (JYFL-ACCLAB) for providing stable online beam. We thank the support by the Academy of Finland under the Finnish Centre of Excellence Programme 2012–2017 (Nuclear and Accelerator Based Physics Research at JYFL) and projects No. 306980, No. 312544, No. 275389, No. 284516, No. 295207, No. 315179, No. 327629, No. 354589, No. 314733, No. 345869, and No. 354968. The support by the EU Horizon 2020 research and innovation program under grant No. 771036 (ERC CoG MAIDEN) is acknowledged. This project has received funding from the European Union’s Horizon 2020 research and innovation programme under grant agreement No. 861198-LISA-H2020-MSCA-ITN-2019. This project has received funding from the European Union’s Horizon Europe Research and Innovation Programme under Grant Agreement No. 101057511 (EURO-LABS). Also the EU-funded NEPTUN project (Project no. CF 264/29.11.2022 of the EU call PNRR-III-C9-2022-I8) is acknowledged.

Funding Open Access funding provided by University of Jyväskylä (JYU).

Data Availability Statement Data will be made available on reasonable request. [Author’s comment: The datasets generated during and/or analysed during the current study are available from the corresponding author on reasonable request.]

Code Availability Statement Code/software will be made available on reasonable request. [Author’s comment: The code/software gen-

erated during and/or analysed during the current study will not be shared/published.]

Open Access This article is licensed under a Creative Commons Attribution 4.0 International License, which permits use, sharing, adaptation, distribution and reproduction in any medium or format, as long as you give appropriate credit to the original author(s) and the source, provide a link to the Creative Commons licence, and indicate if changes were made. The images or other third party material in this article are included in the article’s Creative Commons licence, unless indicated otherwise in a credit line to the material. If material is not included in the article’s Creative Commons licence and your intended use is not permitted by statutory regulation or exceeds the permitted use, you will need to obtain permission directly from the copyright holder. To view a copy of this licence, visit <http://creativecommons.org/licenses/by/4.0/>.

References

- Y. Fukuda, T. Hayakawa, E. Ichihara, K. Inoue, K. Ishihara, H. Ishino, Y. Itow, T. Kajita, J. Kameda, S. Kasuga, K. Kobayashi, Y. Kobayashi, Y. Koshio, M. Miura, M. Nakahata, S. Nakayama, A. Okada, K. Okumura, N. Sakurai, M. Shiozawa, Y. Suzuki, Y. Takeuchi, Y. Totsuka, S. Yamada, M. Earl, A. Habig, E. Kearns, M.D. Messier, K. Scholberg, J.L. Stone, L.R. Sulak, C.W. Walter, M. Goldhaber, T. Barszczak, D. Casper, W. Gajewski, P.G. Halverson, J. Hsu, W.R. Kropp, L.R. Price, F. Reines, M. Smy, H.W. Sobel, M.R. Vagins, K.S. Ganezer, W.E. Keig, R.W. Ellsworth, S. Tasaka, J.W. Flanagan, A. Kibayashi, J.G. Learned, S. Matsuno, V.J. Stenger, D. Takemori, T. Ishii, J. Kanzaki, T. Kobayashi, S. Mine, K. Nakamura, K. Nishikawa, Y. Oyama, A. Sakai, M. Sakuda, O. Sasaki, S. Echigo, M. Kohama, A.T. Suzuki, T.J. Haines, E. Blaufuss, B.K. Kim, R. Sanford, R. Svoboda, M.L. Chen, Z. Conner, J.A. Goodman, G.W. Sullivan, J. Hill, C.K. Jung, K. Martens, C. Mauger, C. Mc Grew, E. Sharkey, B. Viren, C. Yanagisawa, W. Doki, K. Miyano, H. Okazawa, C. Saji, M. Takahata, Y. Nagashima, M. Takita, T. Yamaguchi, M. Yoshida, S.B. Kim, M. Etoh, K. Fujita, A. Hasegawa, T. Hasegawa, S. Hatakeyama, T. Iwamoto, M. Koga, T. Maruyama, H. Ogawa, J. Shirai, A. Suzuki, F. Tsushima, M. Koshiba, M. Nemoto, K. Nishijima, T. Futagami, Y. Hayato, Y. Kanaya, K. Kaneyuki, Y. Watanabe, D. Kielczewska, R.A. Doyle, J.S. George, A.L. Stachyra, L.L. Wai, R.J. Wilkes, K.K. Young, Evidence for oscillation of atmospheric neutrinos. *Phys. Rev. Lett.* **81**(8), 1562–1567 (1998)
- S.N.O. Collaboration, Direct evidence for neutrino flavor transformation from neutral-current interactions in the Sudbury Neutrino Observatory. *Phys. Rev. Lett.* **89**(1), 1–6 (2002)
- G. Martina, L. Massimiliano, Status of neutrino properties and future prospects—cosmological and astrophysical constraints. *Front. Phys.* (2018). <https://doi.org/10.3389/fphy.2017.00070>
- J. Suhonen, O. Civitarese, Weak-interaction and nuclear-structure aspects of nuclear double beta decay. *Phys. Rep.* **300**(3–4), 123–214 (1998)
- F.T. Avignone, S.R. Elliott, J. Engel, Double beta decay, Majorana neutrinos, and neutrino mass. *Rev. Mod. Phys.* **80**(2), 481–516 (2008)
- H. Ejiri, J. Suhonen, K. Zuber, Neutrino-nuclear responses for astro-neutrinos, single beta decays and double beta decays. *Phys. Rep.* **797**, 1–102 (2019)
- C. Velte, F. Ahrens, A. Barth, K. Blaum, M. Braß, M. Door, H. Dorner, Ch.E. Düllmann, S. Eliseev, C. Enss, P. Filianin, A. Fleischmann, L. Gastaldo, A. Goeggelmann, T. Day Goodacre, M.W. Haverkort, D. Hengstler, J. Jochum, K. Johnston, M. Keller, S. Kempf, T. Kieck, C.M. König, U. Köster, K. Kromer, F. Mantegazz-

- ini, B. Marsh, Yu.N. Novikov, F. Piquemal, C. Riccio, D. Richter, A. Rischka, S. Rothe, R.X. Schüssler, Ch. Schweiger, T. Stora, M. Wegner, K. Wendt, M. Zampaolo, K. Zuber, High-resolution and low-background ^{163}Ho spectrum: interpretation of the resonance tails. *Eur. Phys. J. C* **79**(12), 1026 (2019)
8. J.A. Formaggio, A.L.C. de Gouvêa, R.G.H. Robertson, Direct measurements of neutrino mass. *Phys. Rep.* **914**, 1–54 (2021)
 9. E. Ferri, D. Baglioni, M. Biasotti, G. Ceruti, D. Corsini, M. Faverzani, F. Gatti, A. Giachero, C. Gotti, C. Kilbourne, A. Kling, M. Maino, P. Manfrinetti, A. Nucciotti, G. Pessina, G. Pizzigoni, M. Ribeiro Gomes, M. Sisti, The status of the MARE experiment with ^{187}Re and ^{163}Ho isotopes. *Phys. Proc.* **61**(August), 227–231 (2015)
 10. S. Eliseev, K. Blaum, M. Block, S. Chenmarev, H. Dorrer, Ch.E. Düllmann, C. Enss, P.E. Filianin, L. Gastaldo, M. Goncharov, U. Köster, F. Lautenschläger, Yu.N. Novikov, A. Rischka, R.X. Schüssler, L. Schweikhard, A. Türler, Direct measurement of the mass difference of ^{163}Ho and ^{163}Dy solves the Q -value puzzle for the neutrino mass determination. *Phys. Rev. Lett.* **115**(6), 62501 (2015)
 11. P.C.-O. Ranitzsch, C. Hassel, M. Wegner, D. Hengstler, S. Kempf, A. Fleischmann, C. Enss, L. Gastaldo, A. Herlert, K. Johnston, Characterization of the ^{163}Ho electron capture spectrum: a step towards the electron neutrino mass determination. *Phys. Rev. Lett.* **119**, 122501 (2017)
 12. E.G. Myers, A. Wagner, H. Kracke, B.A. Wesson, Atomic masses of tritium and helium-3. *Phys. Rev. Lett.* **114**(1), 013003 (2015)
 13. Schweiger, C., Braß, M., Debierre, V. et al. Penning-trap measurement of the Q value of electron capture in ^{163}Ho for the determination of the electron neutrino mass. *Nat. Phys.* (2024). <https://doi.org/10.1038/s41567-024-02461-9>
 14. M. Aker, K. Altenmüller, M. Arenz, M. Babutzka, J. Barrett, S. Bauer, M. Beck, A. Beglarian, J. Behrens, T. Bergmann, U. Besserer, K. Blaum, F. Block, S. Bobien, K. Bokeloh, J. Bonn, B. Bornschein, L. Bornschein, H. Bouquet, T. Brunst, T.S. Caldwell, L. La Cascio, S. Chilingaryan, W. Choi, T.J. Corona, K. Debowski, M. Deffert, M. Descher, P.J. Doe, O. Dragoun, G. Drexlin, J.A. Dunmore, S. Dyba, F. Edzards, L. Eisenblätter, K. Eitel, E. Ellinger, R. Engel, S. Enomoto, M. Erhard, D. Eversheim, M. Fedkevych, A. Felden, S. Fischer, B. Flatt, J.A. Formaggio, F.M. Fränkle, G.B. Franklin, H. Frankrone, F. Friedel, D. Fuchs, A. Fulst, D. Furse, K. Gauda, H. Gemmeke, W. Gil, F. Glück, S. Görhardt, S. Groh, S. Grohmann, R. Grössle, R. Gumbsheimer, M. Ha Minh, M. Hackenjos, V. Hannen, F. Harms, J. Hartmann, N. Haußmann, F. Heizmann, K. Helbing, S. Hickford, D. Hilk, B. Hillen, D. Hillesheimer, D. Hinz, T. Höhn, B. Holzapfel, S. Holzmann, T. Houdy, M.A. Howe, A. Huber, T.M. James, A. Jansen, A. Kaboth, C. Karl, O. Kazachenko, J. Kellerer, N. Kernert, L. Kippenbrock, M. Kleesiek, M. Klein, C. Köhler, L. Köllenberger, A. Kopmann, M. Korzeczek, A. Kosmider, A. Kovalík, B. Krasch, M. Kraus, H. Krause, L. Kuckert, B. Kuffner, N. Kunka, T. Lasserre, T.L. Le, O. Lebeda, M. Leber, B. Lehnhert, J. Letnev, F. Leven, S. Lichter, V.M. Lobashev, A. Lokhov, M. MacHatschek, E. Malcherek, K. Müller, M. Mark, A. Marsteller, E.L. Martin, C. Melzer, A. Menshikov, S. Mertens, L.I. Minter, S. Mirz, B. Monreal, P.I. Morales Guzmán, K. Müller, U. Naumann, W. Ndeke, H. Neumann, S. Niemes, M. Noe, N.S. Oblath, H.W. Ortjohann, A. Osipowicz, B. Ostrick, E. Otten, D.S. Parno, D.G. Phillips, P. Plischke, A. Pollithy, A.W.P. Poon, J. Pouryamout, M. Prall, F. Priester, M. Röllig, C. Röttele, P.C.O. Ranitzsch, O. Rest, R. Rinderspacher, R.G.H. Robertson, C. Rodenbeck, P. Rohr, S. Ch Roll, M. Rupp, R. Ryšavý, A. Sack, P. Saenz, L. Schäfer, K. Schimpf, M. Schlösser, L. Schlüter, H. Schlüter, K. Schön, M. Schönung, B. Schrank, J. Schulz, H. Schwarz, W. Seitz-Moskaliuk, V. Seller, D. Sibille, A. Siegmann, M. Skasyrskaya, A. Slezák, F. Špalek, M. Spanier, N. Steidl, M. Steinbrink, M. Sturm, M. Suesser, D. Sun, H.H. Tcherniakhovski, T. Telle, L.A. Thümmler, N. Thorne, I. Titov, N. Tkachev, K. Trost, D. Urban, K. Vénos, B.A. Valerius, R. Vandevender, A.P. Vianden, B.L. Vizcaya Hernández, S. Wall, M. Wüstling, C. Weber, C. Weinheimer, S. Weiss, J. Welte, K.J. Wendel, J.F. Wierman, J. Wilkerson, W. Wolf, Y.R. Xu, M. Yen, S. Zacher, M. Zbořil, Zadorozhny, G. Zeller, Improved upper limit on the neutrino mass from a direct kinematic method by Katrin. *Phys. Rev. Lett.* **123**(22), 1–11 (2019)
 15. M. Aker, A. Beglarian, J. Behrens, A. Berlev, U. Besserer, B. Bieringer, F. Block, B. Bornschein, L. Bornschein, M. Böttcher, T. Brunst, T.S. Caldwell, R.M.D. Carney, L. La Cascio, S. Chilingaryan, W. Choi, K. Debowski, M. Deffert, M. Descher, D. Díaz Barrero, P.J. Doe, O. Dragoun, G. Drexlin, K. Eitel, E. Ellinger, R. Engel, S. Enomoto, A. Felden, J.A. Formaggio, F.M. Fränkle, G.B. Franklin, F. Friedel, A. Fulst, K. Gauda, W. Gil, F. Glück, R. Grössle, R. Gumbsheimer, V. Gupta, T. Höhn, V. Hannen, N. Haußmann, K. Helbing, S. Hickford, R. Hiller, D. Hillesheimer, D. Hinz, T. Houdy, A. Huber, A. Jansen, C. Karl, F. Kellerer, J. Kellerer, M. Klein, C. Köhler, L. Köllenberger, A. Kopmann, M. Korzeczek, A. Kovalík, B. Krasch, H. Krause, N. Kunka, T. Lasserre, T.L. Le, O. Lebeda, B. Lehnhert, A. Lokhov, M. Machatschek, E. Malcherek, M. Mark, A. Marsteller, E.L. Martin, C. Melzer, A. Menshikov, S. Mertens, J. Mostafa, K. Müller, S. Niemes, P. Oelpmann, D.S. Parno, A.W.P. Poon, J.M.L. Poyato, F. Priester, M. Röllig, C. Röttele, R.G.H. Robertson, W. Rodejohann, C. Rodenbeck, M. Ryšavý, R. Sack, A. Saenz, P. Schäfer, A. Schaller, L. Schimpf, K. Schlösser, M. Schlösser, L. Schlüter, S. Schneidewind, M. Schrank, B. Schulz, A. Schwemmer, M. Šefčík, V. Sibille, D. Siegmann, M. Slezák, M. Steidl, M. Sturm, M. Sun, D. Tcherniakhovski, H.H. Telle, L.A. Thorne, T. Thümmler, N. Titov, I. Tkachev, K. Urban, K. Valerius, D. Vénos, A.P. Vizcaya Hernández, C. Weinheimer, S. Welte, J. Wendel, J.F. Wilkerson, J. Wolf, S. Wüstling, W. Xu, Y.R. Yen, S. Zadorogny, G. Zeller, Direct neutrino-mass measurement with sub-electron volt sensitivity. *Nat. Phys.* **18**, 160 (2022)
 16. L. Gastaldo, K. Blaum, A. Doerr, Ch.E. Düllmann, K. Eberhardt, S. Eliseev, C. Enss, Amand Faessler, A. Fleischmann, S. Kempf, M. Krivoruchenko, S. Lahiri, M. Maiti, Yu.N. Novikov, P.C.O. Ranitzsch, F. Simkovic, Z. Szusc, M. Wegner, The electron capture ^{163}Ho experiment ECHo. *J. Low Temp. Phys.* **176**(5–6), 876–884 (2014)
 17. L. Gastaldo, K. Blaum, K. Chrysalidis, T. Day Goodacre, A. Domula, M. Door, H. Dorrer, Ch.E. Düllmann, K. Eberhardt, S. Eliseev, C. Enss, A. Faessler, P. Filianin, A. Fleischmann, D. Fonnesu, L. Gamer, R. Haas, C. Hassel, D. Hengstler, J. Jochum, K. Johnston, U. Kebschull, S. Kempf, T. Kieck, U. Köster, S. Lahiri, M. Maiti, F. Mantegazzini, B. Marsh, P. Neroutsos, Yu.N. Novikov, P.C.O. Ranitzsch, S. Rothe, A. Rischka, A. Saenz, O. Sander, F. Schneider, S. Scholl, R.X. Schüssler, F. Ch Schweiger, T. Simkovic, Z. Stora, A. Szűcs, M. Türler, M. Veinhard, M. Weber, K. Wendt, Wegner, K. Zuber, The electron capture in ^{163}Ho experiment—ECHo. *Eur. Phys. J. Spec. Top.* **226**(8), 1623–1694 (2017)
 18. F. Mantegazzini, N. Kovac, C. Enss, A. Fleischmann, M. Griedel, L. Gastaldo, Development and characterisation of high-resolution microcalorimeter detectors for the echo-100k experiment. *Nucl. Instrum. Methods Phys. Res. Sect. A* **1055**, 168564 (2023)
 19. A.A. Esfahani, S. Böser, N. Buzinsky, M.C. Carmona-Benitez, C. Claessens, L. de Viveiros, P.J. Doe, M. Fertl, J.A. Formaggio, J.K. Gaison, L. Gladstone, M. Grando, M. Guigue, J. Hartse, K.M. Heeger, X. Huyan, J. Johnston, A.M. Jones, K. Kazkaz, B.H. LaRoque, M. Li, A. Lindman, E. Machado, A. Marsteller, C. Matthé, R. Mohiuddin, B. Monreal, R. Mueller, J.A. Nikkel, E. Novitski, N.S. Oblath, J.I. Peña, W. Pettus, R. Reimann, R.G.H. Robertson, D. Rosa De Jesús, G. Rybka, L. Saldaña, M. Schram, P.L. Slocum, J. Stachurska, Y.-H. Sun, P.T. Surukuchi, J.R. Tedeschi, A.B. Telles, F. Thomas, M. Thomas, L.A. Thorne, T. Thümmler, L. Tvrznikova, W. Van De Pontseele, B.A. VanDevender, J. Weintrob, T.E. Weiss, T. Wendler, A. Young, E. Zayas,

- A. Ziegler, Tritium beta spectrum measurement and neutrino mass limit from cyclotron radiation emission spectroscopy. *Phys. Rev. Lett.* **131**, 102502 (2023)
20. A. Nucciotti, B. Alpert, M. Balata, D. Becker, D. Bennett, A. Bevilacqua, M. Biasotti, V. Ceriale, G. Ceruti, D. Corsini, M. De Gerone, R. Dressler, M. Faverzani, E. Ferri, J. Fowler, G. Gallucci, J. Gard, F. Gatti, A. Giachero, J. Hays-Wehle, S. Heinitz, G. Hilton, U. Köster, M. Lusignoli, J. Mates, S. Nisi, A. Orlando, L. Parodi, G. Pessina, A. Puiu, S. Ragazzi, C. Reintsema, M. Ribeiro-Gomez, D. Schmidt, D. Schuman, F. Siccardi, D. Swetz, J. Ullom, L. Vale, Status of the HOLMES experiment to directly measure the neutrino mass. *J. Low Temp. Phys.* **193**(5–6), 1137–1145 (2018)
 21. M. Borghesi, B. Alpert, M. Balata, D. Becker, D. Bennet, E. Celasco, N. Cerboni, M. De Gerone, R. Dressler, M. Faverzani, M. Fedkevych, E. Ferri, J. Fowler, G. Gallucci, J. Gard, F. Gatti, A. Giachero, G. Hilton, U. Koster, D. Labranca, M. Lusignoli, J. Mates, E. Maugeri, S. Nisi, A. Nucciotti, L. Origo, G. Pessina, S. Ragazzi, C. Reintsema, D. Schmidt, D. Schumann, D. Swetz, J. Ullom, L. Vale, An updated overview of the Holmes status. *Nucl. Instrum. Methods Phys. Res. Sect. A* **1051**, 168205 (2023)
 22. M.T. Mustonen, J. Suhonen, Nuclear and atomic contributions to beta decays with ultra-low Q values. *J. Phys. G: Nucl. Part. Phys.* **37**(6), 64008 (2010)
 23. M.T. Mustonen, J. Suhonen, Theoretical analysis of the possible ultra-low-q-value decay branch of ^{135}Cs . *Phys. Lett. B* **703**(3), 370–375 (2011)
 24. M. Haaranen, J. Suhonen, Beta decay of ^{115}Cd and its possible ultra-low Q-value branch. *Eur. Phys. J. A* **49**(7), 1–9 (2013)
 25. J. Suhonen, Theoretical studies of rare weak processes in nuclei. *Phys. Scr.* **89**(5), 54032 (2014)
 26. National Nuclear Data Center. Available at <https://www.nndc.bnl.gov>. Accessed 20 December 2023 (2023)
 27. M. Wang, W.J. Huang, F.G. Kondev, G. Audi, S. Naimi, The AME 2020 atomic mass evaluation (II). tables, graphs and references. *Chin. Phys. C* **45**(3), 030003 (2021)
 28. W.J. Huang, M. Wang, F.G. Kondev, G. Audi, S. Naimi, The AME 2020 atomic mass evaluation (I). Evaluation of input data, and adjustment procedures. *Chin. Phys. C* **45**(3), 030002 (2021)
 29. R. Sandler, G. Bollen, N.D. Gamage, A. Hamaker, C. Izzo, D. Puentes, M. Redshaw, R. Ringle, I. Yandow, Investigation of the potential ultralow Q-value β -decay candidates Sr 89 and Ba 139 using Penning trap mass spectrometry. *Phys. Rev. C* **100**(2), 1–5 (2019)
 30. J. Karthein, D. Atanasov, K. Blaum, S. Eliseev, P. Filianin, D. Lunney, V. Manea, M. Mougeot, D. Neidherr, Y. Novikov, L. Schweikhard, A. Welker, F. Wienholtz, K. Zuber, Direct decay-energy measurement as a route to the neutrino mass. *Hyperfine Interact.* **240**(1), 1–9 (2019)
 31. A. De Roubin, J. Kostensalo, T. Eronen, L. Canete, R.P. De Groote, A. Jokinen, A. Kankainen, D.A. Nesterenko, I.D. Moore, S. Rinta-Antila, J. Suhonen, M. Vilén, High-precision Q-value measurement confirms the potential of Cs 135 for absolute antineutrino mass scale determination. *Phys. Rev. Lett.* **124**(22), 1–5 (2020)
 32. Z. Ge, T. Eronen, A. de Roubin, D.A. Nesterenko, M. Hukkanen, O. Beliuskina, R. de Groote, S. Geldhof, W. Gins, A. Kankainen, Á. Koszorús, J. Kotila, J. Kostensalo, I.D. Moore, A. Raggio, S. Rinta-Antila, J. Suhonen, V. Virtanen, A.P. Weaver, A. Zadvornaya, A. Jokinen, Direct measurement of the mass difference of $^{72}\text{As} - ^{72}\text{Ge}$ rules out ^{72}As as a promising β -decay candidate to determine the neutrino mass. *Phys. Rev. C* **103**, 065502 (2021)
 33. Z. Ge, T. Eronen, K.S. Tyrin, J. Kotila, J. Kostensalo, D.A. Nesterenko, O. Beliuskina, R. de Groote, A. de Roubin, S. Geldhof, W. Gins, M. Hukkanen, A. Jokinen, A. Kankainen, Á. Koszorús, M.I. Krivoruchenko, S. Kujanpää, I.D. Moore, A. Raggio, S. Rinta-Antila, J. Suhonen, V. Virtanen, A.P. Weaver, A. Zadvornaya, ^{159}Dy electron-capture: a new candidate for neutrino mass determination. *Phys. Rev. Lett.* **127**, 272301 (2021)
 34. T. Eronen, Z. Ge, A. de Roubin, M. Ramalho, J. Kostensalo, J. Kotila, O. Beliuskina, C. Delafosse, S. Geldhof, W. Gins, M. Hukkanen, A. Jokinen, A. Kankainen, I.D. Moore, D.A. Nesterenko, M. Stryjczyk, J. Suhonen, High-precision measurement of a low q value for allowed beta-decay of ^{131}I related to neutrino mass determination. *Phys. Lett. B* **830**, 137135 (2022)
 35. Z. Ge, T. Eronen, A. de Roubin, K.S. Tyrin, L. Canete, S. Geldhof, A. Jokinen, A. Kankainen, J. Kostensalo, J. Kotila, M.I. Krivoruchenko, I.D. Moore, D.A. Nesterenko, J. Suhonen, M. Vilén, High-precision electron-capture q value measurement of ^{111}In for electron-neutrino mass determination. *Phys. Lett. B* **832**, 137226 (2022)
 36. Z. Ge, T. Eronen, A. de Roubin, J. Kostensalo, J. Suhonen, D.A. Nesterenko, O. Beliuskina, R. de Groote, C. Delafosse, S. Geldhof, W. Gins, M. Hukkanen, A. Jokinen, A. Kankainen, J. Kotila, Á. Koszorús, I.D. Moore, A. Raggio, S. Rinta-Antila, V. Virtanen, A.P. Weaver, A. Zadvornaya, Direct determination of the atomic mass difference of the pairs $^{76}\text{As} - ^{76}\text{Se}$ and $^{155}\text{Tb} - ^{155}\text{Gd}$ rules out ^{76}As and ^{155}Tb as possible candidates for electron (anti)neutrino mass measurements. *Phys. Rev. C* **106**, 015502 (2022)
 37. M. Ramalho, Z. Ge, T. Eronen, D.A. Nesterenko, J. Jaatinen, A. Jokinen, A. Kankainen, J. Kostensalo, J. Kotila, M.I. Krivoruchenko, J. Suhonen, K.S. Tyrin, V. Virtanen, Observation of an ultralow-q-value electron-capture channel decaying to ^{75}As via a high-precision mass measurement. *Phys. Rev. C* **106**, 015501 (2022)
 38. N.D. Gamage, R. Sandler, F. Buchinger, J.A. Clark, D. Ray, R. Orford, W.S. Porter, M. Redshaw, G. Savard, K.S. Sharma, A.A. Valverde, Precise q-value measurements of $^{112,113}\text{Ag}$ and ^{115}Cd with the canadian penning trap for evaluation of potential ultralow q-value β decays. *Phys. Rev. C* **106**, 045503 (2022)
 39. D.K. Kebelbeck, R. Bhandari, N.D. Gamage, M Horana Gamage, K.G. Leach, X. Mougeot, M. Redshaw, Updated evaluation of potential ultralow q-value β -decay candidates. *Phys. Rev. C* **107**, 015504 (2023)
 40. M. Redshaw, Precise q value determinations for forbidden and low energy $\beta\beta$ -decays using penning trap mass spectrometry. *Eur. Phys. J. A* **59**(2), 18 (2023)
 41. Z. Ge, T. Eronen, A. de Roubin, M. Ramalho, J. Kostensalo, J. Kotila, J. Suhonen, D.A. Nesterenko, A. Kankainen, P. Ascher, O. Beliuskina, M. Flayol, M. Gerbaux, S. Grévy, M. Hukkanen, A. Husson, A. Jaries, A. Jokinen, I.D. Moore, P. Pirinen, J. Romero, M. Stryjczyk, V. Virtanen, A. Zadvornaya, β^- decay q-value measurement of ^{136}Cs and its implications for neutrino studies. *Phys. Rev. C* **108**, 045502 (2023)
 42. D.A. Nesterenko, L. Canete, T. Eronen, A. Jokinen, A. Kankainen, Yu.N. Novikov, S. Rinta-Antila, A. de Roubin, M. Vilén, High-precision measurement of the mass difference between ^{102}Pd and ^{102}Ru . *Int. J. Mass Spectrom.* **435**, 204–208 (2019)
 43. T. Eronen, J.C. Hardy, High-precision Q_{EC} -value measurements for superallowed decays. *Eur. Phys. J. A* **48**(4), 1–8 (2012)
 44. V.S. Kolhinen, T. Eronen, D. Gorelov, J. Hakala, A. Jokinen, K. Jokiranta, A. Kankainen, M. Koikkalainen, J. Koponen, H. Kulmala, M. Lantz, A. Mattera, I.D. Moore, H. Penttilä, T. Pikkarainen, I. Pohjalainen, M. Reponen, S. Rinta-Antila, J. Rissanen, C. Rodriguez Triguero, K. Rytkönen, A. Saastamoinen, A. Solders, V. Sonnenschein, J. Äystö, Recommissioning of JYFLTRAP at the new IGISOL-4 facility. *Nucl. Instrum. Methods Phys. Res. Sect. B Beam Interact. Mater. Atoms* **317**(Part B), 506–509 (2013)
 45. I.D. Moore, T. Eronen, D. Gorelov, J. Hakala, A. Jokinen, A. Kankainen, V.S. Kolhinen, J. Koponen, H. Penttilä, I. Pohjalainen, M. Reponen, J. Rissanen, A. Saastamoinen, S. Rinta-Antila, V. Sonnenschein, J. Äystö, Towards commissioning the new IGISOL-

- 4 facility. Nucl. Instrum. Methods Phys. Res. Sect. B **317**(PART B), 208–213 (2013)
46. J. Huikari, P. Dendooven, A. Jokinen, A. Nieminen, H. Penttilä, K. Peräjärvi, A. Popov, S. Rinta-Antila, J. Äystö, Production of neutron deficient rare isotope beams at IGISOL; on-line and off-line studies. Nucl. Instrum. Methods Phys. Res. Sect. B **222**(3–4), 632–652 (2004)
47. P. Karvonen, I.D. Moore, T. Sonoda, T. Kessler, H. Penttilä, K. Peräjärvi, P. Ronkanen, J. Äystö, A sextupole ion beam guide to improve the efficiency and beam quality at IGISOL. Nucl. Instrum. Methods Phys. Res. Sect. B **266**(21), 4794–4807 (2008)
48. A. Nieminen, J. Huikari, A. Jokinen, J. Äystö, P. Campbell, E.C.A. Cochrane, Beam cooler for low-energy radioactive ions. Nucl. Instrum. Methods Phys. Res. Sect. A **469**(2), 244–253 (2001)
49. G. Savard, St. Becker, G. Bollen, H.J. Kluge, R.B. Moore, Th. Otto, L. Schweikhard, H. Stolzenberg, U. Wiess, A new cooling technique for heavy ions in a Penning trap. Phys. Lett. A **158**(5), 247–252 (1991)
50. D.A. Nesterenko, T. Eronen, Z. Ge, A. Kankainen, M. Vilen, Study of radial motion phase advance during motion excitations in a penning trap and accuracy of jyfltrap mass spectrometer. Eur. Phys. J. A **57**, 302 (2021)
51. D.A. Nesterenko, T. Eronen, A. Kankainen, L. Canete, A. Jokinen, I.D. Moore, H. Penttilä, S. Rinta-Antila, A. de Roubin, M. Vilen, Phase-imaging ion-cyclotron-resonance technique at the JYFLTRAP double Penning trap mass spectrometer. Eur. Phys. J. A **54**(9), 0–13 (2018)
52. S. Eliseev, K. Blaum, M. Block, A. Dörr, C. Droese, T. Eronen, M. Goncharov, M. Höcker, J. Ketter, E. Minaya Ramirez, D.A. Nesterenko, Yu.N.N. Novikov, L. Schweikhard, A phase-imaging technique for cyclotron-frequency measurements. Appl. Phys. B Lasers Opt. **114**(1–2), 107–128 (2014)
53. M. Kretzschmar, A quantum mechanical model of Rabi oscillations between two interacting harmonic oscillator modes and the interconversion of modes in a Penning trap. AIP Conf. Proc. **457**(1), 242–251 (1999)
54. A. Kramida, Yu.Ralchenko, J. Reader, NIST ASD Team. NIST Atomic Spectra Database (ver. 5.8), [Online]. Available: <https://physics.nist.gov/asd> [2021, January 19] (National Institute of Standards and Technology, Gaithersburg, MD) (2020)
55. C. Roux, K. Blaum, M. Block, C. Droese, S. Eliseev, M. Goncharov, F. Herfurth, E.M. Ramirez, D.A. Nesterenko, Y.N. Novikov, L. Schweikhard, Data analysis of Q-value measurements for double-electron capture with SHIPTRAP. Eur. Phys. J. D **67**(7), 1–9 (2013)
56. A. Kellerbauer, K. Blaum, G. Bollen, F. Herfurth, H.J. Kluge, M. Kuckein, E. Sauvan, C. Scheidenberger, L. Schweikhard, From direct to absolute mass measurements: a study of the accuracy of ISOLTRAP. Eur. Phys. J. D **22**(1), 53–64 (2003)
57. R.T. Birge, The calculation of errors by the method of least squares. Phys. Rev. **40**(2), 207–227 (1932)
58. G. Engler, R.E. Chrien, H.I. Liou, Thermal and resonance neutron capture studies in se targets with $a = 74, 76, 77, 78, 80$. Nucl. Phys. A **372**(1), 125–140 (1981)
59. Y. Tokunaga, H. Seyfarth, R.A. Meyer, O.W.B. Schult, H.G. Börner, G. Barreau, H.R. Faust, K. Schreckenbach, S. Brant, V. Paar, M. Vouk, D. Vretenar, Low-lying levels of ^{77}Se studied by thermal neutron capture and evidence for a new term in the $e2$ operator of rqm (ibm). Nucl. Phys. A **439**(3), 427–455 (1985)
60. R.B. Firestone, H.D. Choi, R.M. Lindstrom, G.L. Molnar, S.F. Mughabghab, R. Paviotti-Corcuera, Zs. Revay, A. Trkov, C.M. Zhou, V. Zerkin, Database of prompt gamma rays from slow neutron capture for elemental analysis, vol. 12 (2004)
61. N. Shimizu, T. Mizusaki, Y. Utsuno, Y. Tsunoda, Thick-restart block lanczos method for large-scale shell-model calculations. Comput. Phys. Commun. **244**, 372–384 (2019)
62. M. Honma, T. Otsuka, T. Mizusaki, M. Hjorth-Jensen, New effective interaction for $f_{5/2}g_{9/2}$ -shell nuclei. Phys. Rev. C **80**(6), 064323 (2009)
63. S. Mukhopadhyay, B.P. Crider, B.A. Brown, S.F. Ashley, A. Chakraborty, A. Kumar, M.T. McEllistrem, E.E. Peters, F.M. Prados-Estévez, S.W. Yates, Nuclear structure of Ge^{76} from inelastic neutron scattering measurements and shell model calculations. Phys. Rev. C **95**(1), 014327 (2017)
64. O. Nițescu, S. Stoica, F. Šimkovic, Exchange correction for allowed β decay. Phys. Rev. C **107**, 025501 (2023)